Available online at www.sciencedirect.com
SCIENCE DIRECT®
Polymer 44 (2003) 8147–8154
polymer
www.elsevier.com/locate/polymer

Polymer/silicate nanocomposites synthesized with potassium persulfate at room temperature: polymerization mechanism, characterization, and mechanical properties of the nanocomposites

Yeong Suk Choi, Hyeong Taek Ham, In Jae Chung*

Department of Chemical and Biomolecular Engineering, Korea Advanced Institute of Science and Technology (KAIST), 373-1, Guseong-dong, Yuseong-gu, Daejeon, South Korea

Received 26 June 2003; received in revised form 28 August 2003; accepted 8 October 2003

Abstract

Polymer/silicate nanocomposites were synthesized using potassium persulfate (KPS) in the presence of silicate and 2-acrylamido-2-methyl-1-propanesulfonic acid (AMPS) without exterior redox co-catalysts at a room temperature. A mechanism for the room temperature polymerization in the presence of silicate was suggested: AMPS attached on the surface of silicate layers would oxidize Fe^{+2} in silicate lattice to become Fe^{+3} and the Fe^{+3} would decompose KPS to form radicals like redox co-catalysts. Poly (acrylonitrile) (PAN)/silicate nanocomposite showed an exfoliated structure, but poly (methyl methacrylate) (PMMA)/silicate nanocomposite showed an intercalated structure. Polymers recovered from the nanocomposites synthesized at a room temperature had high isotactic configurations compared to bulk polymers. The dipole–dipole interaction between monomers and silicate surface might make the lamella of monomers to form on the silicate layer surface and produced polymers with more isotactic configurations. PAN/silicate nanocomposite showed two glass transition temperatures at 113 and 151 °C. The lower temperature might be related to the molecules with low molecular weight. PMMA/silicate nanocomposite had a storage modulus of 4.47×10^9 Pa at 40 °C.

Keywords: Silicate; Nanocomposites; Room temperature polymerization

1. Introduction

Catalytic role or catalyst supporters of silicates [1–7] had been recognized a few decades ago. Some of them showed spontaneous polymerizations of monomers in presence of silicates. Friedlander reported spontaneous polymerization of butadiene adsorbed in interlayer spaces of neutral or acid montmorillonites. Solomon reported that hydroxyethyl methacrylate (HEMA) complex with reduced montmorillonites spontaneously polymerized without any initiators because the electron-donating sites in the silicates initiated polymerization through radical-anions mechanism. Pinnavia demonstrated that protonated amines in clay activated the polymerization of epoxy, because the acidity of amines affected the rate of polymerization. While Blumstein polymerized monomer/montmorillonite complexes using free-radical initiator or photo-polymerization, and the resultant polymers showed higher isotactic configuration than pure polymer. The change in catalytic activity of silicate or in tacticity of polymers due to silicate was much related with monomers confined in the interlayer spaces of silicates except olefin. Even though the molecular weights of the resultant polymers except the epoxy were low for mechanical applications, they showed the basic concepts of polymer/silicate nanocomposites [20–27]. From other perspectives, silicates could imbibe catalysts and initiated monomers to make polymer/silicate nanocomposites [22–24]. The catalytic activity of silicates [8–10] may result from the metal ions in the lattice or the dipolar nature of aluminum oxide. Smectite clays have generally two tetrahedral sheets, silicon oxides, and one octahedral sheet, aluminum oxides, in a layer. Other metal ions such as Fe^{+2}, Mn^{+2} can be included in the silicate layer due to imperfection of unit lattice. So, we can expect clays as catalytic activity materials or catalyst supporters like silica [11,12].

* Corresponding author. Tel.: +82-42-869-3916; fax: +82-42-869-3910.
E-mail address: chung@kaist.ac.kr (I.J. Chung).

0032-3861/$ - see front matter © 2003 Elsevier Ltd. All rights reserved.
doi:10.1016/j.polymer.2003.10.041

We observed a catalytic activity of silicate in emulsion polymerization without exterior redox co-catalysts at a room temperature. When a free-radical initiator, potassium persulfate (KPS), added into the mixture of sodium montmorillonite and monomers in aqueous media at room temperature, polymerizations occurred to form polymer/silicate nanocomposites under certain conditions. One of polymer/silicate nanocomposites showed exfoliated structure. The merit of room temperature polymerization will be to produce polymers having peculiar tacticity portions through a cost-saving process. In this paper, we will examine the behavior of polymerization at room temperature and mechanical properties of the polymer/silicate nanocomposites, and then we will suggest a mechanism for the polymerization.

2. Experimental section

2.1. Materials

Acrylonitrile (AN), methyl methacrylate (MMA), and 2-acrylamido-2-methyl-1-propanesulfonic acid (AMPS) [16–18] were purchased from Aldrich and used as received. The silicate we used in this paper was sodium montmorillonite (Na-MMT) of Kunipia-F purchased from Kunimine Co. and the silicate had 119 mequiv./100 g of cation exchange capacity. Pristine silicate was dispersed in deionized water for 24 h at an ambient temperature, before use. Potassium persulfate (KPS) of Junsei, a radical initiator, was recrystallized using deionized water. *N*,*N*-Dimethylformamide (DMF) and tetrahydrofuran (THF) of HPLC solvent grade were used as received from Fluka for poly (acrylonitrile) (PAN) and poly (methyl methacrylate) (PMMA) recovery in reverse ionexchange. Methyl alcohol (MeOH: Fluka) and *n*-hexane (Junsei), nonsolvents for PAN and PMMA, were distilled at a normal pressure. Lithium chloride (LiCl, Junsei) was recrystallized with tetrahydrofuran (THF).

2.2. Synthesis of polymer/silicate nanocomposites at room temperature

Polymerization of AN or MMA with the silicate was carried out in the following method. For example, aqueous silicate dispersion containing 5 wt% of silicate to monomer, 200 g of deionized water, 2-acrylamido-2-methyl-1-propanesulfonic acid (AMPS = 0.3 g), and 20 g of monomer were charged into a 1000 ml four-neck glass reactor fitted with a condenser, a rubber septum, and a nitrogen inlet, and the reactor was stirred with a magnetic spin bar at 100 rpm to disperse the mixture for 1 h under nitrogen atmosphere at 25 °C. 20 g of KPS (1 wt% aqueous solution), stored in a refrigerator to avoid thermal decomposition, was added into to the reactor and stirred for 3 days. White particles in the reactor were generated after 10–30 min of KPS addition. After the completion of polymerization, polymer/silicate nanocomposites were recovered by a freeze–drying method for 5 days.

2.3. Polymer recovery by reverse ion exchange [34]

PAN and PMMA were recovered from the polymer/silicate nanocomposites in the following ways and then were subjected to measure molecular weight and tacticity using GPC and NMR.

PMMA/silicate nanocomposite (about 0.2 g) was dispersed in 80 ml of THF for 2 h to which LiCl of 0.3 g was added and stirred for 5 days at ambient temperature. The mixture was centrifuged at 6000 rpm for 30 min to separate the molecules from the silicate cakes. Transparent solution was filtered with a 0.45 μm membrane filter and poured into *n*-hexane (10–20 folds) to precipitate PMMA. The precipitated polymer was filtered and dried in a high vacuum at 80 °C for 50 h.

PAN/silicate nanocomposite (about 0.1 g) was extracted with DMF/LiCl solution (60 g/0.2 g = DMF/LiCl) under a nitrogen atmosphere at 80 °C for 5 days in a 500 ml three-neck reactor fitted with a condenser, a nitrogen inlet and outlet. The mixture was centrifuged at 10,000 rpm for 30 min to separate polymers from the silicate cakes. The extract was filtered with a 0.45 μm membrane filter to remove clays or unwanted particles and poured into MeOH (10–20 folds) to precipitate PAN. The precipitated polymer was filtered and dried in a high vacuum at 80 °C for 50 h. Its molecular weight was measured with GPC.

2.4. Measurements

X-ray diffraction patterns were obtained by using a Rigaku X-ray generator (Cu Kα with $\lambda = 0.15406$) at a room temperature with a scanning rate of 2°/min in the 2θ range of 1.5–10°. Nanocomposites for X-ray diffraction patterns were prepared in a shape of disk under a pressure of 3000 psi. Number average molecular weight of PAN was determined by using GPC performed at a flow rate of DMF 1.0 ml/min at 80 °C using a Polymer Laboratories 220 GPC system equipped with three styragel columns (500, two 10^6) and a RID detector after calibration with 10 polystyrene standards obtained from Easical Co. Number average molecular weight of PMMA was determined by using a Waters R-401 ALC/GPC equipped with six styragel HR columns (two 500, two 10^3, 10^4, and 10^5) and a Water 410 RID detector after calibration with 10 PMMA standards obtained from Polymer Laboratories at a flow rate of THF 2.0 ml/min at room temperature.

Thermogravimetric analyses (TGA) were carried out with a Perkin–Elmer thermobalance by heating from room temperature to 600 °C with a scan rate of 10 °C/min under N_2 atmosphere.

tan δ and storage modulus (E') were obtained by a Rheometric Scientific DMTA4 with a dual cantilever from

30 to 200 °C with a heating rate of 5 °C/min under 0.07% deformation for PMMA and 0.04% deformation for PAN at 1 Hz of frequency, respectively. Samples were molded in $1 \times 28 \times 1.2\ mm^3$ size at 140 °C for 2 minutes under a pressure of 3000 psi. The glass transition temperatures, T_g, were determined from maximum values in the tan δ vs. temperature scans.

^{1}H NMR spectrum of PMMA was collected using a Bruker DMX 600 spectrometer employing acetone as the solvent. ^{13}C NMR spectrum of PAN was collected using a Bruker DRX 300 spectrometer employing DMSO as the solvent at 80 °C.

Chemical composition of pristine silicate was collected using an electron probe micro-analyzer (EPMA) SX-51 of CAMECA. Before EPMA measurements, pristine silicate was pre-dried to remove waters adsorbed naturally under a high vacuum at a room temperature and molded in a shape of disk at 3000 psi for 4 min. The accelerating voltage, the beam current, and the beam diameter were 15 kV, 10 nA and 20 μm, respectively. The counting time was 10 s on the peak positions of elements after 10 s of background counting.

A UV–visible spectrometer of Cray 40 equipped with a magnetic stirrer and a thermal controller was used to measure the absorbance of PAN during polymerization at 25 °C. Deionized water (5 g), aqueous silicate dispersion (0.037 g), AN (0.074 g), and AMPS (0.037 g) were added to a standard quartz cell and stirred at 100 rpm with a spin bar. After baseline correction and zeroing with the mixture, the absorbance of the mixture was measured, soon after aqueous KPS solution (0.037 g) was charged into the mixture under a scan rate of 1 nm/s within a wavelength range of 220–800 nm.

Infrared spectra were recorded on a Bomem 102 Fourier Transform Infrared spectrometer (FT-IR) with KBR pellets. A total of 40 scans taken at 4 cm^{-1} of resolutions were averaged.

The morphology of the nanocomposite was examined by a Philips CM-20 transmission electron microscope (TEM). The nanocomposite was sliced in 100 nm thickness and coated with carbon. The accelerating voltage of TEM was 160 kV.

3. Results

We choose two monomers, methyl methacrylate (MMA) and acrylonitrile (AN), having different degrees of dipole strength, because these dipolar monomers will easily gather on hydrophilic silicate layers and that will enhance probability of polymerization near the silicates. Table 1 shows polymerization conditions and yields of polymer/silicate nanocomposites. Polymerizations were commenced at a room temperature, when all of AMPS, silicate, and initiator (KPS) are included. The yields of PAN and PMMA/silicate nanocomposites calculated from residual amounts in TGA measurements are 100 and 71%, respectively. The residues of bulk PAN and PMMA under the same condition in TGA measurement are 61 and 3%, respectively [26,27]. AN shows much higher yield than MMA, since AN has a higher dipole strength than MMA, the polarity of AN may affect the yield of polymerization. From now on, we omit the number 1 next to PAN and PMMA. The half-life of KPS at 35 °C in aqueous media is 1600 h [28] and the thermal decomposition rate of KPS is affected by addition of chemicals such as $KHSO_4$, or metal cations (Fe^{+2}) changing the ionic strength of the media [28]. Therefore the addition of silicate and AMPS will affect the polymerization with KPS.

Fig. 1 shows X-ray diffraction patterns of (b) PMMA/silicate nanocomposite and (c) PAN/silicate nanocomposite in the range of 1.2–10°. PMMA/silicate nanocomposite shows a broad peak at around 5.0°, indicating an intercalated morphology with its d_{001} spacing of 1.76 nm. PAN/silicate nanocomposite shows no peak, indicating exfoliated state.

Fig. 2 exhibits ^{13}C NMR spectrum of PAN (a) and ^{1}H NMR spectrum of PMMA (b) recovered from the nanocomposites by reverse ion exchange. In Fig. 2(a), methylene carbon (CH_2) peaks of PAN show at 27.7–28.7δ, methine carbon (CH) at 33.6–34.0δ, and cyante carbon (C≡N) at 120–121δ, which are the typical carbon peaks of PAN. Tacticity of PAN is calculated using the peak areas at 28.7δ for isotactic, at 28.3δ for heterotactic, and at 27.7δ for syndiotactic configurations of methylene carbon (CH_2).

In Fig. 2(b), methoxy protons (O–CH_3) of MMA show a peak at 3.6δ and methylene protons (CH_2) show peaks in the range of around 2.2–1.5δ. A peak at 1.27δ is for isotactic, at 1.04δ for heterotactic, and at 0.8δ for syndiotactic configuration of α-methyl protons (CH_3) in PMMA. Those peaks are typical spectrum of PMMA. Unfortunately, peaks of AMPS are not discernible in those peaks because the amount of AMPS is very small. The tacticity of polymers obtained from Fig. 2(a) and (b) is listed in Table 2. PAN has 32.0% of isotactic, 19.9% of syndiotactic, and

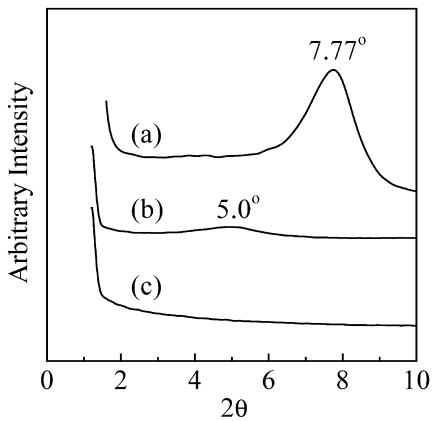

Fig. 1. X-ray diffraction patterns of polymer/silicate nanocomposites and pristine silicate (Na-MMT): (a) pristine silicate, a reference and its pattern is measured by the powder method, (b) PMMA/silicate nanocomposite, and (c) PAN/silicate nanocomposite.

Table 1
Polymerization conditions and yields

Test number	Monomers and weight charged (g)	AMPS (g)	Silicate (wt% to monomer)	KPS (g)	Yield (%)[a]
PMMA1	MMA, 20 g	0.3	5	0.2	71
PMMA2	MMA, 20 g	0.3	5	None	No polymz.
PMMA3	MMA 20 g	0.3	None	0.2	No polymz.
PMMA4	MMA, 20 g	None	5	0.2	No polymz.
PAN1	AN, 20 g	0.3	5	0.2	100
PAN2	AN, 20 g	0.3	5	None	No polymz.
PAN3	AN, 20 g	0.3	None	0.2	No polymz.
PAN4	AN, 20 g	None	5	0.2	No polymz.

[a] The residues of bulk PAN and PMMA under the same condition in TGA measurement are about 61 and 3%, respectively.

48.1% of heterotactic configurations. PMMA shows 17.4% of isotactic, 54.5% of syndiotactic, and 28.1% of heterotactic configurations. PAN from the nanocomposites synthesized at room temperature has more isotactic and less syndiotactic configurations than PAN synthesized through anionic polymerization at −78 °C by Masatomo Minagawa and co-workers [14,15]. PMMA recovered from PMMA/silicate nanocomposite has more isotactic and less heterotactic configurations than bulk PMMA initiated by γ-rays. Alexandre Blumstein and co-workers [13] reported that they polymerized the lamella of MMA adsorbed in interlayer space of silicate using free-radical initiators or γ-rays, and the resultant PMMA exhibited more isotactic configuration than bulk polymers synthesized without silicates. The enhanced isotactic configurations in PAN and PMMA synthesized with the silicate at room temperature may result from the polymerization of monomers on silicate layers like template reaction. The monomers penetrate into the galleries of silicate layers and form the lamellar on the silicate layers by the dipole–dipole interaction between monomers and silicate surface. Therefore, the polymers with more isotactic configuration are produced.

Fig. 3 shows UV–visible absorbance of PAN/silicate nanocomposite during polymerization. Soon after the addition of the initiator, KPS, to a quartz containing the mixture of AMPS, AN, and silicate, the intensity due to the absorbance of PAN increase at around 240–340 nm wavenumber range, and it strongly indicates that polymerization by KPS occurs in the presence of AMPS and silicate. While polymerization is not carried out without silicate, the absorbance curve is omitted for simplicity.

Table 2
Tacticity dependence on polymers from various sources

Polymers	P_i (%)	P_s (%)	P_h (%)	Initiation
PAN bulk[a]	30	27	43	Anion −78 °C
PAN	32.0	19.9	48.1	KPS, room temperature with silicate
PMMA bulk[b]	5	56	39	γ-rays 30 °C
Monolayer[b]	35	26	39	BPO 60 °C
PMMA	17.4	54.5	28.1	KPS, room temperature with silicate

[a] Tacticity percent of PAN calculated by Masatomo Minagawa and co-workers [14,15].

[b] Tacticity percent obtained by Alexandre Blumstein and co-workers [13]. P_i, P_s, and P_h stand for the percent of isotactic, syndiotactic, and heterotactic configurations calculated using the area of each tacticity and sum of all α-methyl proton peak areas for PMMA, and methylene carbon peak areas for PAN, respectively.

The chemical composition of pristine silicate may give clues to explain this polymerization mechanism. Table 3 shows a little amount of divalent metal ions, Fe^{+2}, Mn^{+2}, implanted in a unit cell of the silicate. The amounts of MgO, FeO, and MnO are 3.297, 1.955, and 0.012% in compounds, respectively. These divalent metal ions cause the charge deficiency by replacing Al^{+3} in the octahedral sheets of silicates and attract monovalent metal ions on the silicate layer, such as Na^{+}. We focus on the amount of Fe^{+2} in the silicate, because it can donate an electron to the environment when it is oxidized to become Fe^{+3}.

Fig. 4 shows the mechanism we suggest. In an aqueous media, AMPS dissociates a proton in the sulfonic acid. The proton moves to nitrogen to form a protonated amido portion and exchange with sodium ions on silicates. The sodium dissociated from silicates will associate with sulfate ion of AMPS to form sulfonic acid sodium salt, a polar portion of surfactants. The AMPS will move to the surface of silicate layers due to the dipolar interaction [19], and will make the Fe^{+2} in silicate lattice oxidize to become Fe^{+3} after release one electron. The electron will decompose the initiator to form radicals like redox initiation systems [28]. High yield of PAN compared to PMMA also supports the mechanism, because more AN monomers are bound to silicate layers by the strong negative cyanate groups than MMA monomers bound by the carbonyl group.

Table 4 shows the molecular weights of PAN and PMMA extracted from the nanocomposites. Number-average molecular weights (M_n) of PAN and PMMA were 280,000 and 232,000, respectively. The polydisperisity index (PDI = M_w/M_n) of PAN and PMMA are broad. The difference of PAN and PMMA in molecular weight may involve the polarity of monomers and the yield of polymers, since AN is more polar than MMA, and hydrophilic sodium montmorillonite interacts with the monomers through various mechanisms based on dipole interactions [33] which means that the silicate will adsorb monomers proportional

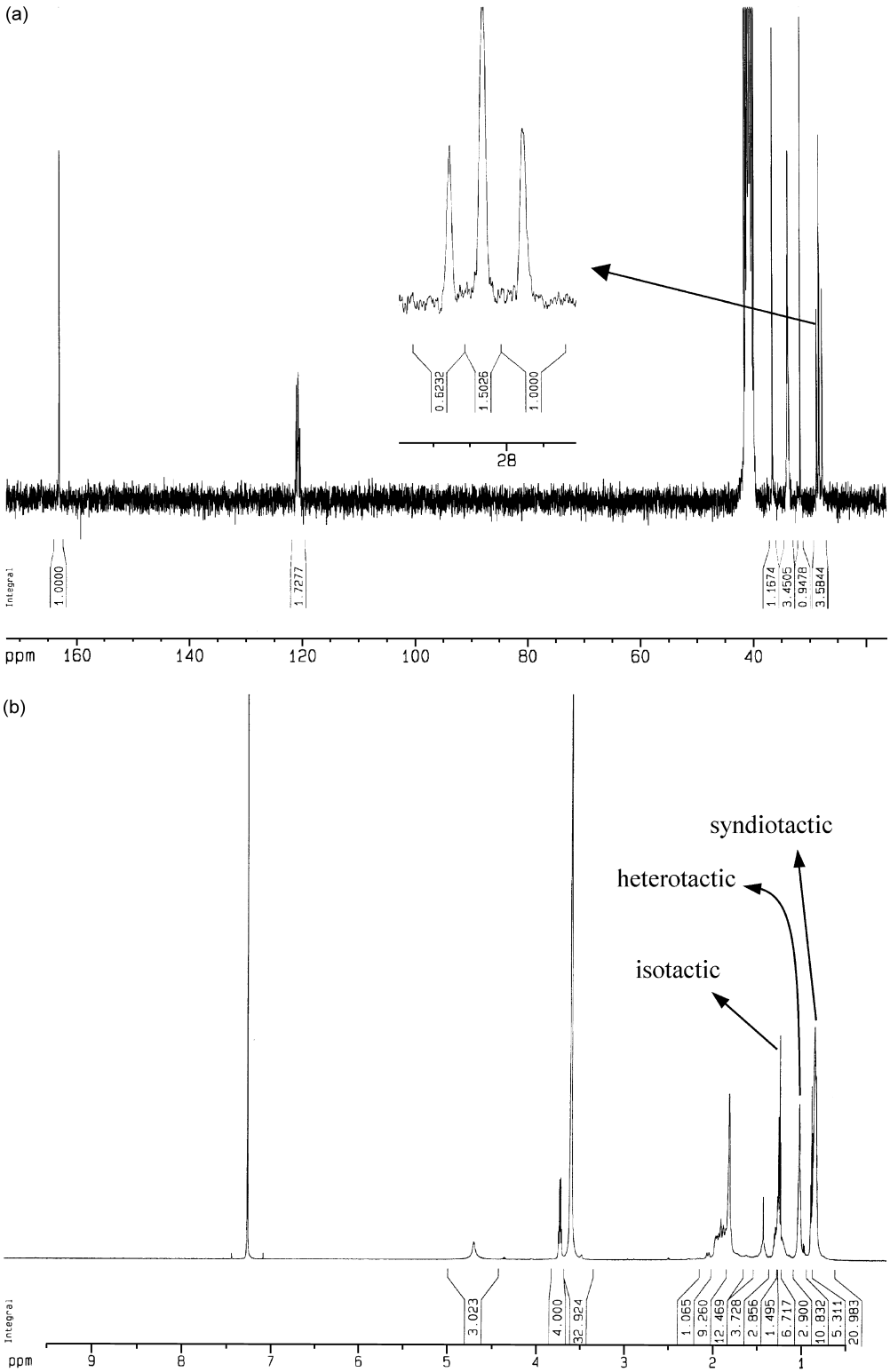

Fig. 2. ^{13}C NMR spectrum of (a) PAN retrieved from PAN/silicate nanocomposite, and ^{1}H NMR spectrum of (b) PMMA retrieved from PMMA/silicate nanocomposite by the reverse ion exchange.

to polarities of the monomers, and the rate of polymerization become fast, as more monomers are adsorbed on the silicate. This is the reason why PAN has higher molecular weight with broad PDI than that of PMMA.

Fig. 5 shows thermogravimetric analysis (TGA) of the nanocomposites as a function of weight loss. Thermal decomposition of PAN main chain occurs at about 361–460 °C. In the temperature range of 500–600 °C, the residue

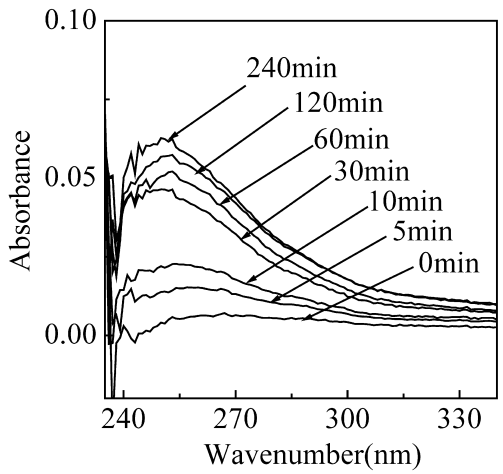

Fig. 3. Time-resolved UV–visible absorbance spectra of PAN/silicate nanocomposite.

reaches the weight percentage of 61–34% of the original nanocomposite. The PAN/silicate nanocomposite shows the higher residual content than PMMA/silicate nanocomposite because of the formation of ring compounds, pyridinoid structures. PMMA commences the thermal decomposition in the range of 181–376 °C and the thermal degradation of its main chain in the range of 376–489 °C. Transformation of PAN to pyridinoid structures after TGA measurement was checked using FT-IR in Fig. 5(b). Three new absorbance bands at about 1620–1500 (C=C stretching), 1380–1267 (C=N stretching), and 790 cm^{-1} (C–H out of plane) indicated the conversion of linear polymer chains in PAN into pyridinoid structures [29–32].

PAN/silicate nanocomposite shows a storage modulus at 40 °C, 3.43×10^9 Pa in Fig. 6. PAN/silicate nanocomposite has two glass transition temperatures, T_g, at 113 and 151 °C, and the lower temperature may be related to low molecules

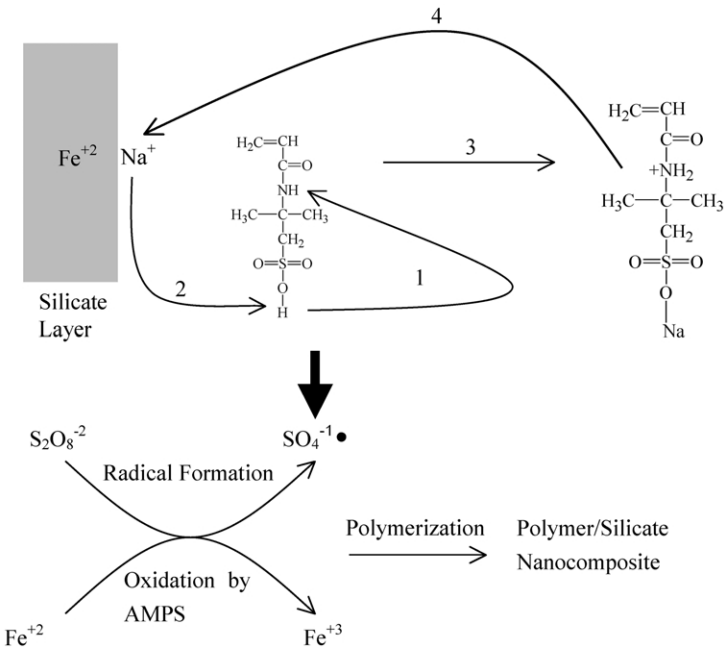

Fig. 4. Schematic description of polymerization at a room temperature with silicate.

Table 3
Chemical composition of pristine silicate (Na-MMT) obtained by EPMA

Run No.	Na_2O	SiO_2	Al_2O_3	MgO	P_2O_5	K_2O	CaO	TiO_2	FeO	MnO	Total
1	3.258	59.367	21.711	3.247	0.007	0.066	0.371	0.163	1.964	0.000	90.159
2	3.460	59.787	21.976	3.397	0.000	0.100	0.396	0.087	1.925	0.010	91.142
3	3.611	60.394	22.029	3.391	0.027	0.098	0.648	0.152	2.012	0.031	92.397
4	3.645	60.698	22.301	3.305	0.007	0.098	0.193	0.118	1.939	0.000	92.307
5	3.509	59.376	22.010	3.233	0.023	0.130	0.627	0.135	1.914	0.000	90.961
6	3.522	59.156	21.711	3.223	0.016	0.108	0.796	0.148	2.020	0.006	90.712
7	3.595	59.926	22.378	3.348	0.000	0.071	0.624	0.122	1.971	0.000	92.037
8	3.521	58.899	22.110	3.273	0.000	0.119	0.666	0.132	1.934	0.000	90.657
9	3.428	59.085	21.641	3.286	0.018	0.082	0.936	0.177	1.868	0.043	90.568
10	3.404	60.026	21.687	3.321	0.007	0.134	0.248	0.117	1.989	0.000	90.936
11	3.336	59.710	21.507	3.240	0.018	0.064	0.606	0.115	1.967	0.043	90.610
Average	3.481	59.675	21.915	3.297	0.011	0.097	0.556	0.133	1.955	0.012	91.135

Table 4
Molecular weights of polymers recovered from polymer/silicate nanocomposites synthesized at a room temperature

Polymers retrieved from nanocomposites	M_n	M_w	PDI (M_w/M_n)
PAN	280,000	2,253,000	8.04
PMMA	232,000	1,203,000	5.18

in the composite. PMMA/silicate nanocomposite shows a storage modulus of 4.47×10^9 Pa at 40 °C. PMMA has a glass transition temperature, T_g, at around 151 °C.

TEM is used to confirm the morphology of PAN/silicate nanocomposite in Fig. 7, in which silicate layers look like dark strips, and PAN appears as bright domains. Delaminated layers of silicate are well distributed in entire PAN matrix.

4. Conclusion

Polymer/silicate nanocomposites were synthesized using KPS in the presence of silicate and AMPS without exterior redox co-catalysts at a room temperature. The yields of PAN and PMMA/silicate nanocomposites calculated from the residual amounts in TGA measurements are 100 and 71%, respectively. The diffraction pattern of PMMA/silicate nanocomposite due to (001) planes of silicate occurs at 5.0°, showing an intercalated morphology, and its d_{001} spacing is 1.76 nm. The diffraction pattern of PAN/silicate nanocomposite is not visible, indicating the exfoliated state. PAN and PMMA from the nanocomposites synthesized at a room temperature have more isotactic and less syndiotactic or heterotactic configurations than bulk polymers because the silicate layers function as a template. PAN has 32.0% of isotactic, 19.9% of syndiotactic, and 48.1% of heterotactic configuration. PMMA has 17.4% of isotactic, 54.5% of syndiotactic, and 28.1% of heterotactic configurations. The chemical composition of pristine silicate shows a little amount of divalent metal ions, Fe^{+2}, Mn^{+2}, are implanted in the unit cell of silicate. We propose a mechanism of the

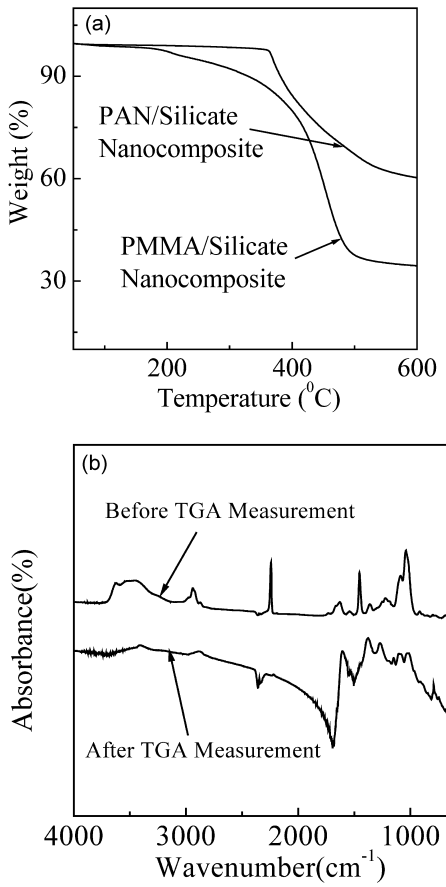

Fig. 5. (a) Thermal gravimetric curves for polymer/silicate nanocomposites synthesized at a room temperature. (b) FT-IR spectra of PAN/silicate nanocomposite before and after TGA measurements.

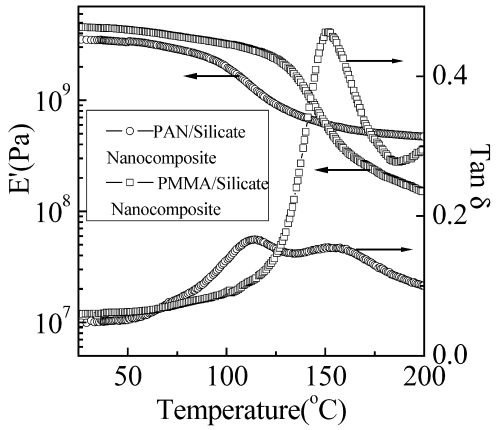

Fig. 6. Storage moduli and tan δ of PAN and PMMA/silicate nanocomposites.

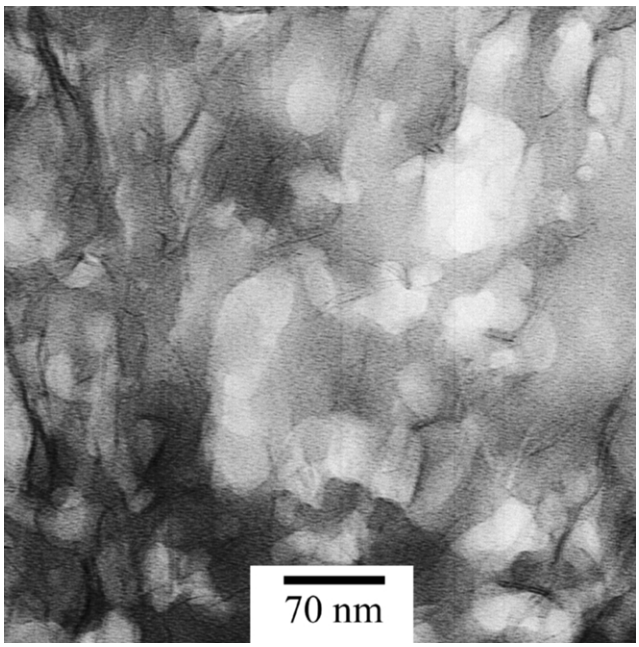

Fig. 7. TEM micrograph of PAN/silicate nanocomposite.

room temperature polymerization with silicate: AMPS will oxidize Fe^{+2} into Fe^{+3} and the divalent ion, Fe^{+2}, will release an electron. The electron will decompose the initiator, KPS, through redox initiation systems. Number-average molecular weights (M_n) of PAN and PMMA were 280,000 and 232,000, respectively. For PAN/silicate nanocomposite, storage modulus, E', at 40 °C is 3.43×10^9 Pa and PAN has two glass transition temperatures at 113 and 151 °C. For PMMA/silicate nanocomposite, storage modulus at 40 °C is 4.47×10^9 Pa and its glass transition temperature, T_g, occurs at 151 °C.

Acknowledgements

Authors would like to express the sincere thanks to Korea Science and Engineering Foundation (KOSEF), Center for Advanced Functional Polymers (CAFPoly), and BK 21 program for their financial support.

References

[1] Friedlander HZ, Fink CR. J Polym Sci B 1964;2:475.
[2] Solomon DH, Rosser MJ. J Appl Polym Sci 1965;9:1261.
[3] Friedlander HZ. J Polym Sci 1963;4:1291.
[4] Blumstein A. J Polym Sci A 1965;3:2653.
[5] Soloman DH, Loft BC. J Appl Polym Sci 1968;12:1253.
[6] Lan T, Kaviratna PD, Pinnavaia TJ. J Phys Chem Solids 1995;57:1005.
[7] Moet AS, Akelah A. Mater Lett 1993;18:97.
[8] Pinnavaia TJ. Science 1983;220:365.
[9] Kinrade SD, Nin JWD, Schach AS, Sloan TA, Wilson KL, Knight CTG. Science 1999;285:1542.
[10] Flockhart BD, Naccache C, Scott JAN, Pink RC. Chem Commun 1965;238.
[11] Jarupatrakorn J, Tilly TD. J Am Chem Soc 2002;124:8380.
[12] Choi CH, Gordon MS. J Am Chem Soc 2002;124:6162.
[13] Blumstein A, Malhotra SL, Watterson AC. J Polym Sci Polym Phys 1970;8:1599.
[14] Minagawa M, Miyano K, Takahashi M. Macromolecules 1988;21:2387.
[15] Minagawa M, Miyano K, Morita T, Yoshii F. Macromolecules 1989;22:2054.
[16] Seki M, Morishima Y, Kamachi M. Macromolecules 1992;25:6540.
[17] Morishima Y, Nomura S, Ikeda T, Seki M, Kamachi M. Macromolecules 1995;28:2874.
[18] Aota H, Akaki SI, Morishima Y, Kamachi M. Macromolecules 1997;30:4090.
[19] Cannizaro CE, Houk KN. J Am Chem Soc 2002;124:7163.
[20] Croce F, Appetecchi GB, Persi L, Scrosati B. Nature 1998;394:456.
[21] Byun HY, Choi MH, Chung IJ. Chem Mater 2001;13:4221.
[22] Leu CM, Wu ZW, Wei KH. Chem Mater 2002;14:3016.
[23] Weimer MW, Chen H, Giannelis EP, Sogah DY. J Am Chem Soc 1999;121:1615.
[24] Bergman JS, Chen H, Giannelis EP, Thomas MG, Coates GW. Chem Commun 1999;2179.
[25] Marestin C, Guyot A, Claverie J. Macromolecules 1998;31:1686.
[26] Choi YS, Choi MH, Wang KY, Kim SO, Kim YK, Chung IJ. Macromolecules 2001;34:8978.
[27] Choi YS, Wang KH, Xu M, Chung IJ. Chem Mater 2002;14:2936.
[28] Blackley DC. Emulsion Polymerization Theory Practice 1982;163.
[29] Ko TH, Huang LC. J Appl Polym Sci 1998;70:2409.
[30] Thünemann A, Ruland W. Macromolecules 2000;33:2626.
[31] Thünemann A, Ruland W. Macromolecules 2000;33:1848.
[32] Viswanathan H, Wang YQ, Audi AA, Allen PJ, Sherwood PMA. Chem Mater 2001;13:1647.
[33] Giese RF, van Oss CJ. Colloid and surface properties of clays and related minerals. 2002. p. 54.
[34] Messersmith PB, Giannelis EP. J Polym Sci Polym Chem 1995;33:1047.